GEOPHYSICS, VOL. 63, NO. 6 (NOVEMBER-DECEMBER 1998); P. 1947–1957, 11 FIGS.

Depth to magnetic source using the generalized analytic signal

Shu-Kun Hsu*, Dorothée Coppens‡, and Chuen-Tien Shyu**

ABSTRACT

The advantage of using analytic signal techniques to determine magnetic parameters from magnetic anomalies is the independence of magnetization direction. In addition, using the amplitude ratio method to determine depths to magnetic sources can avoid tedious operations with several characteristic points and reduce interference effects. A drawback of this method, however, is the assumption that near-surface structures can be characterized adequately by step models. To improve mapping resolution, we have extended the amplitude ratio method to allow both step-like and dike-like structures. A criterion is constructed that discriminates between maxima from dike-like or step-like structures and significantly improves near-surface structural mapping. This avoids a bias in geological interpretation caused by the original assumption that all structures can be characterized by step models. Synthetic data and real data acquired offshore northern Taiwan demonstrate the effectiveness of this method.

INTRODUCTION

The analytic signal, which is a complex function and makes use of Hilbert transform properties, has been shown to be effective in interpreting subsurface magnetic contacts (e.g., Nabighian, 1972, 1974). This method does not require knowledge of magnetization directions and thus does not require reduction-to-the-pole processing. A geologic contact or fault with significant susceptibility contrast is detected by mapping the maxima of the simple analytic signal, which is composed of the two horizontal and one vertical gradients (Nabighian, 1972, 1974, 1984; Roest et al., 1992). It is typically assumed that the causative sources are near-vertical, step-like geologic structures (Nabighian, 1972; Roest et al., 1992; Hsu et al., 1996b), in which case the maxima are located directly over the edges of the structures. An interpretation pitfall of using this method is that two maxima from two nearby parallel edges merge to one maximum if the half-width between the edges is less than the depth (Atchuta Rao et al., 1981). Consequently, a dike could be interpreted as a geologic fault or contact. This problem could be mitigated somewhat by acquiring the magnetic data close to or on the ground. However, this is often impractical. An alternative and easier way is to increase the resolution by introducing high-order vertical derivatives (Marson and Klingele, 1993; Hsu et al., 1996b) or continuing downward the magnetic data. However, the latter is less stable than the former (Nabighian, 1974). The application of the high-order vertical derivatives can enhance the resolution and reduce the inherent interference effect (Hsu et al., 1996b) if smooth and high-quality data are used.

The depth to the top surface of a step-like or dike-like structure can be estimated by using the amplitude–distance relationship between the center of the characteristic bell-shaped function (of the simple analytic signal) and a certain horizontal position—for example, where the half-amplitude or the inflection point occurs (Nabighian, 1972; MacLeod et al., 1993). The depth parameter can also be determined by doing a least-squares fit between the measured analytic signal and its theoretical bell-shaped function (Roest et al., 1992). On the other hand, several methods based on characteristic points have been developed to estimate the depth and width of an isolated dike-like structure without interfering anomalies (e.g., Atchuta Rao et al., 1981; Murthy, 1985; Sundararajan et al., 1985). However, in the 3-D case those procedures become complicated because of varying strikes of the structures and interfering anomalies.

Using the amplitude ratio method to determine the magnetic parameters of a step-like structure was first introduced by Hsu et al. (1996b). This approach provides the advantage of using only the maxima to estimate the magnetic parameters. Using the peak values of the bell-shaped functions of analytic signals suffers less interference than using the values of the flanks, and the processing is significantly simplified. The amplitude ratio method lends itself more easily to mapping near-surface structures in addition to interpreting along a profile. In this paper, we extend the concept introduced by Hsu et al. (1996b) by developing the amplitude ratio relationship for dike-like structures and proposing an algorithm recognizing the attributes of the

Manuscript received by the Editor May 13, 1996; revised manuscript received January 16, 1998.
*Institute of Geophysics, National Central University, Chung-Li, Taiwan.
‡Institut de Physique du Globe, CNRS URA323, 67084 Strasbourg, France; presently Jet Propulsion Laboratory, Pasadena, California 91109.
**Institute of Oceanography, National Taiwan University, P.O. Box 23-13, Taipei, Taiwan.

analytic signal maxima. Because using a different initial model would result in different depth estimates (e.g., Debeglia and Corpel, 1997), this improvement is necessary and important in two key ways: (1) finding more adequate forms to reflect the magnetic sources and (2) increasing the accuracy of depth estimation.

THEORETICAL FORMULATION

For a magnetic anomaly G, the generalized (simple and enhanced) analytic signal (for integer $n \geq 0$) is defined in Hsu et al. (1996b) as

$$A_n(x, y) = \frac{\partial}{\partial x}(\nabla^n G)\hat{x} + \frac{\partial}{\partial y}(\nabla^n G)\hat{y} + i\frac{\partial}{\partial z}(\nabla^n G)\hat{z}, \quad (1)$$

where $\nabla^n = \partial^n/\partial z^n$ and $\nabla^0 = 1$. Its amplitude is defined as

$$|A_n(x, y)| = \sqrt{\left[\frac{\partial}{\partial x}(\nabla^n G)\right]^2 + \left[\frac{\partial}{\partial y}(\nabla^n G)\right]^2 + \left[\frac{\partial}{\partial z}(\nabla^n G)\right]^2}. \quad (2)$$

Step model with infinite thickness

For a 2-D step-like structure with the variables shown in Figure 1a, the magnetic anomaly G can be written in the form (Nabighian, 1972)

$$G(x) = \alpha\left[(\theta_1 - \theta_2)\cos\Phi + \sin\Phi\,\ell n\,\frac{r_1}{r_2}\right], \quad (3)$$

where $\alpha = 2kFc\sin\theta$; $c = 1 - \cos^2 i \sin^2 A$ for total-field magnetic anomaly; $\Phi = 2I - \theta - 90°$ for total-field magnetic anomaly; k is the susceptibility contrast; F is the earth's magnetic field; i is the inclination of the earth's magnetic field; A is the angle between magnetic north and the positive x axis; and $\tan I = \tan i / \cos A$.

If we let thickness t in Figure 1a approach infinity, the amplitude of generalized analytic signal [equation (2)] for a step-like structure in the 3-D case is (Hsu et al., 1996b)

$$|A_n(x, y)| = \frac{n!|\alpha|}{\sqrt{(d^2 + h^2)^{n+1}}}, \quad (4)$$

where h is the horizontal projection of x onto the direction perpendicular to the strike of the step model (Figure 1b), i.e., $h = x\cos\Psi$, where Ψ is the angle between the x axis and the direction perpendicular to the strike of the step model. In the 2-D case, equation (4) becomes $|A_n(x)| = n!\,|\alpha|/\sqrt{(d^2 + x^2)^{n+1}}$. Because we are interested only in using the maxima to estimate the magnetic parameters, we hereafter will express the theoretical values at the center of each maximum (i.e., $x = 0$). To restrain high-frequency noise amplication, we will use only the order $n = 0, 1, 2$. Hence, the maximum of the bell-shaped function [equation (4)] is located directly over the edge of the step-like structure and corresponds to

$$|A_n(0)| = \frac{n!|\alpha|}{d^{n+1}}. \quad (5)$$

From equation (5) and for the order $n = 0, 1, 2$, the depth d can be estimated in three ways:

$$d = \frac{1}{c_1}, \quad (6)$$

$$d = \sqrt{\frac{2}{c_2}}, \quad (7)$$

or

$$d = \frac{2c_1}{c_2}, \quad (8)$$

where

$$c_1 = \left|\frac{A_1(0)}{A_0(0)}\right| \quad \text{and} \quad c_2 = \left|\frac{A_2(0)}{A_0(0)}\right|.$$

Estimation of depth from equations (6), (7), or (8) is valid only when the bottom surface of the step model is at infinity.

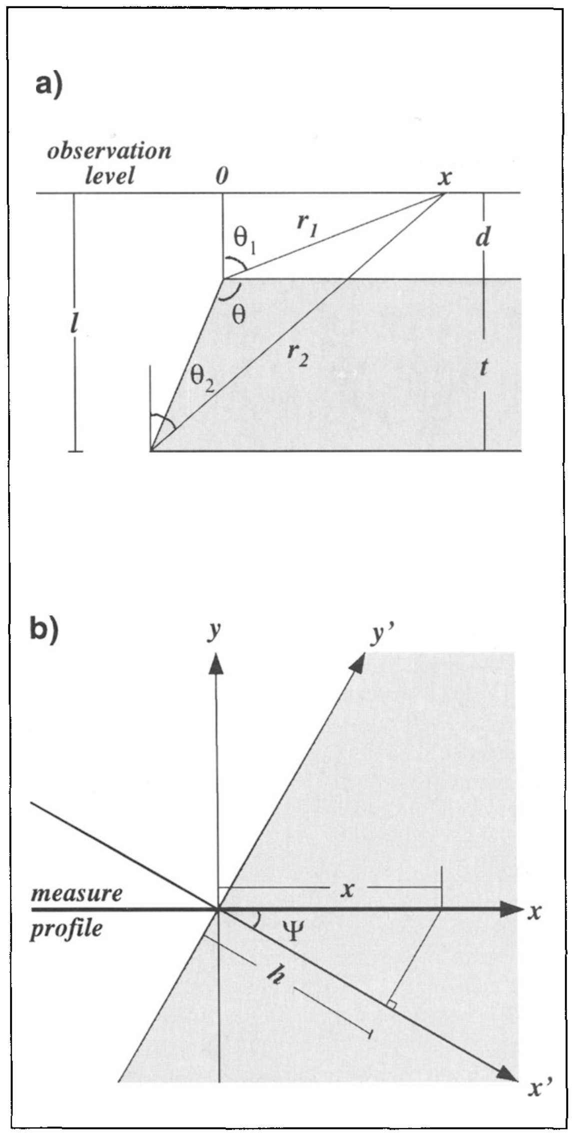

FIG. 1. (a) Cross-sectional view of a step model. (b) Plane view of the step model whose strike is along the y'-direction, but the survey is supposed to be conducted along the x-direction.

Obviously, this assumption is not realistic and some error in depth estimation will result. The error generally decreases as the thickness t increases; higher order analytic signal ratios are generally less sensitive to finite thickness (Figure 2). From our experience, it is appropriate to adopt the average depth estimated from equations (7) and (8), accounting for error from numerical approximation.

Vertical step model with finite thickness

If the above step model has a finite thickness t and its dipping angle is vertical (i.e., $\theta = 90°$), then its maximum amplitude remains centered over the edge and is given by the difference between a shallow infinite step with depth d and a deep infinite step with depth ℓ (Figure 1a). Hence,

$$|A_n(0)| = n!\left(\frac{1}{d^{n+1}} - \frac{1}{\ell^{n+1}}\right)|\alpha|. \quad (9)$$

The unknown parameters d and ℓ could be solved by using equation (9) for the order $n = 0, 1, 2$; hence,

$$d = \frac{c_1 - \sqrt{2c_2 - 3c_1^2}}{2c_1^2 - c_2} \quad (10)$$

and

$$\ell = \frac{d}{c_1 d - 1}, \quad (11)$$

where

$$c_1 = \left|\frac{A_1(0)}{A_0(0)}\right| \quad \text{and} \quad c_2 = \left|\frac{A_2(0)}{A_0(0)}\right|.$$

Meaningful solutions of equation (10), i.e., $d > 0$, require that $2c_2 - 3c_1^2 > 0$. In other words, the maxima are not because of a near-vertical step-like structure when $2c_2 - 3c_1^2 < 0$. Estimating depths d of an isolated near-vertical, step-like structure from equation (10) is more accurate than depths estimated from equations (6), (7), or (8). However, estimation from equation (10) becomes less accurate when interference from an adjacent edge increases. The estimation of depth ℓ is not very stable because of the inherent problem of S/N ratio. High-order derivatives amplify noise. This is why we only use the generalized analytic signal of the order $n = 0, 1, 2$, which provides the minimum requirements to solve the three parameters in equation (9). Otherwise, more simultaneous equations, comprised of different orders, could be used to estimate more magnetic parameters in equation (3).

Dike model

A dike model is frequently used in magnetic interpretation. Because the potential field data represent the superposition of effects from different causative sources, a dike model can be regarded as the difference between two parallel step models with a fixed horizontal offset. With the variables shown in Figure 3, the amplitude of the simple analytic signal (i.e., $n = 0$) caused by a dike with its strike perpendicular to the x-direction is

$$|A_0(x)| = \frac{2w|\alpha|}{\sqrt{[d^2 + (x - w)^2][d^2 + (x + w)^2]}}. \quad (12)$$

To find the maximum amplitude of equation (12), we solve for x when $\partial|A_0(x)|/\partial x = 0$. Thus,

$$x = 0 \qquad \text{if } w \le d \quad (13)$$

or

$$x = \pm\sqrt{w^2 - d^2} \qquad \text{if } w > d. \quad (14)$$

Equations (13) and (14) show that a dike model with a half-width w has a resolution limit of d in the case of the simple analytic signal. For $d \ge w$, the $|A_0(x)|$ curve corresponds to a bell-shaped function with one maximum. For $d < w$, the $|A_0(x)|$ curve has two maxima located equal distances on either side of the origin. The distance (or mislocation) for each maximum from the adjacent edge of the dike is $|w - \sqrt{w^2 - d^2}|$ (see also Atchuta Rao et al., 1981). The amplitude of the first-order enhanced analytic signal (i.e., $n = 1$) is

$$|A_1(x)| = \frac{4w\sqrt{(x^2 + d^2)}|\alpha|}{[d^2 + (x - w)^2][d^2 + (x + w)^2]}. \quad (15)$$

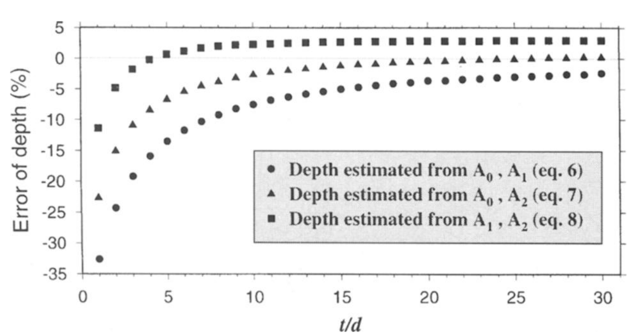

FIG. 2. Plot of the ratio of thickness t to depth d below the observation level versus estimation error of depth d existing in a vertical step model. The depths are calculated from equations (6), (7), and (8), respectively. The error of estimation generally decreases as the thickness t increases.

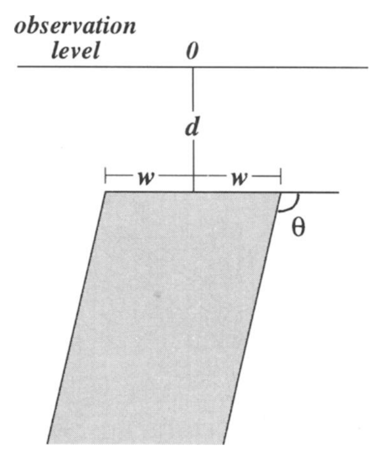

FIG. 3. Cross-sectional view of a dike model. A dike is regarded as thin dike when the maxima used for determining the magnetic parameters are all centered over the dike. A limiting case is geologic contact ($w \to \infty$); each edge of the dike corresponds to a step model.

The maximum amplitudes occur at

$$x = 0 \qquad \text{if } w \leq \sqrt{2\sqrt{3} - 3}d(\approx 0.68d) \tag{16}$$

or

$$x = \pm\sqrt{\frac{(w^2 - 3d^2) + 2w\sqrt{w^2 + 3d^2}}{3}}$$

$$\text{if } w > \sqrt{2\sqrt{3} - 3}d. \tag{17}$$

Equations (12) through (17) show that the analytic signal amplitudes are symmetric about the center of a dike and are independent of the dipping angle θ. The first-order enhanced analytic signal resolves into two peaks when $w > 0.68d$, whereas the simple analytic signal resolves into two peaks when $w > d$. Hence, the resolvable width of a dike and the mislocation from each edge of the dike are considerably reduced when a higher order of the analytic signal is used. When half-width w approaches infinity, the mislocation approaches zero. For convenience, we define a dike-like structure as a thin dike when only one maximum is centered over the dike for each order of analytic signal used to determine the parameters. The analytic signal amplitudes for $n = 0, 1, 2$ at the center of a dike are

$$|A_0(0)| = \frac{2w|\alpha|}{d^2 + w^2}, \tag{18}$$

$$|A_1(0)| = \frac{4wd|\alpha|}{(d^2 + w^2)^2}, \tag{19}$$

and

$$|A_2(0)| = \left|\frac{4w(3d^2 - w^2)\alpha}{(d^2 + w^2)^3}\right|. \tag{20}$$

The depth d and half-width w of a dike model can therefore be estimated from

$$d = \frac{c_1}{2c_1^2 - c_2} \tag{21}$$

and

$$w = \sqrt{\frac{2d}{c_1} - d^2}, \tag{22}$$

where

$$c_1 = \left|\frac{A_1(0)}{A_0(0)}\right| \quad \text{and} \quad c_2 = \left|\frac{A_2(0)}{A_0(0)}\right|.$$

Equation (22) shows that if $w < 0$, the peak is not centered over a dike-like structure. In this case, a step model should be used for estimating depth d associated with the peak. As for the estimation of the dipping angle θ for a dike-like or step-like structure, apparently it cannot be obtained by analyzing the amplitudes of analytic signal. A phase term should be involved, i.e., the relationship between the horizontal and vertical derivatives should be used (e.g., Atchuta Rao et al., 1981; Thurston and Smith, 1997).

SYNTHETIC EXAMPLES

To compute the amplitudes of the generalized analytic signal from potential field anomalies, a numerical approximation can be used (e.g., Hsu et al., 1996b). For an isolated magnetic source, the earlier formulations for determining the parameters of step or dike models are completely valid. But interference of anomalies is inevitable in real data. We demonstrate in the following sections how interference influences the determination of magnetic parameters when the proposed amplitude ratio method is applied. Although parameter α can be estimated using the amplitude relationship, there is no information about its mathematical sign, and it consists of several variables that cannot be separated easily. For example, if a step model is rotated clockwise about its corner or is comprised of two different sources (Figure 4), the peak of the analytic signal is always directly above the corner but the value of parameter α changes from one case to the other. This is because the models in Figures 4b and 4c can be considered to be the superposition of two or several step models that have the same corner. The

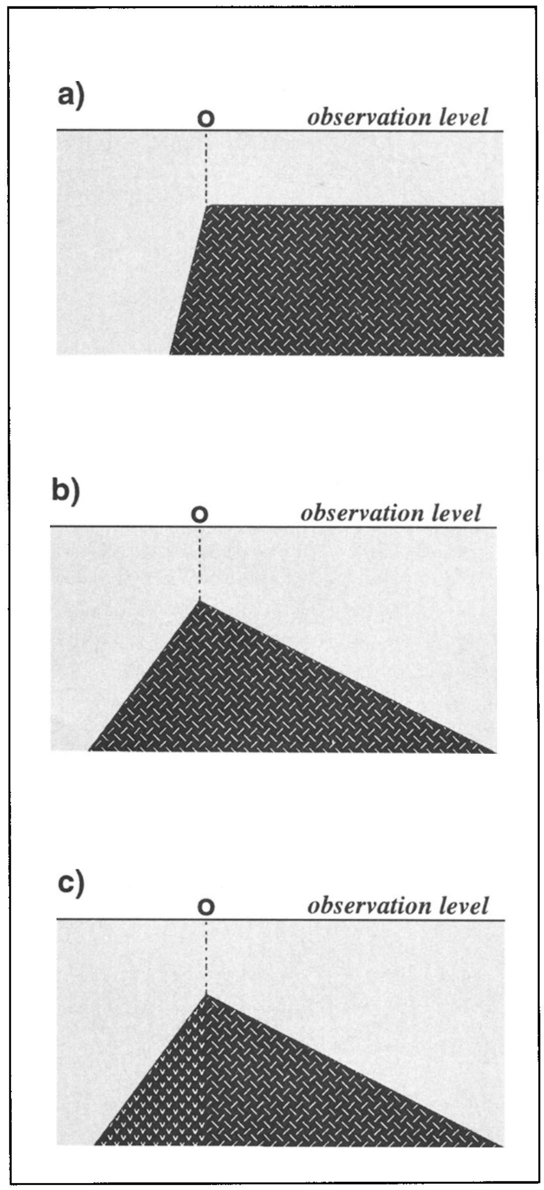

FIG. 4. Schematic examples showing a constant depth but variable ambient parameter α. (a) A typical step model. (b) A step model rotated clockwise. (c) A rotated step model comprised of two different sources.

maxima of A_0, A_1, and A_2 usually are not at the same locations; however, the discrepancy in depth estimation is limited if we use the amplitudes of A_0 and A_1 at the locations defined by the maxima of A_2 (Hsu et al., 1996b). The estimation is more accurate if the magnetization contrast for the structure is larger. However, we must pay attention to the high-frequency error. If necessary, a high-cut filter should be used before applying the proposed method, which could result in overdetermining somewhat the depth of magnetic boundaries.

Interference effect for step and thin-dike models

To demonstrate the interference effect, we first estimate the magnetic parameters for vertical step and thin-dike models separated by distance ℓ (Figure 5). For a grid spacing of 0.2 km, the amplitudes of analytic signals for the order $n = 0, 1, 2$ are shown in the upper part of Figure 5. Now we vary the distance ℓ and estimate the magnetic parameters from amplitudes A_0, A_1, and A_2. As expected, the results are better when the interference effect is decreased (i.e., the distance ℓ increases; Figure 6). In general, the parameter determination of a dike-like structure is more sensitive to interference than a step-like structure.

Dike models with varying width

We now consider dike models with widths varying from 1 to 7 km (Figure 7). The depth to the top surface of each dike is 2 km, while the bottom surfaces are at infinity. The distance between dikes is 20 km, which means interference between dikes is not important. The analytic signals for the order $n = 0, 1, 2$, calculated with a grid spacing of 0.2 km, are shown in the upper part of Figure 7. When width $2w$ is <2 km, the amplitudes present only one peak over the center of the dike. When the width of the dike increases, two peaks corresponding to two edges of each dike appear. The analytic signal of higher order better resolves two maxima. The edge of a rather wide dike model can be regarded as the edge of a step model with infinite bottom. The question is how we can attribute an analytic signal maximum to a dike or to a step model, especially when a dike is not very narrow nor very wide (e.g., $2w = 3$ km or $2w = 4$ km). In this case, the attribution of a maximum becomes ambiguous in the sense that two peaks appear in the higher order analytic signal (e.g., $n = 2$) but only one peak appears in the lower order (e.g., $n = 0$) because of different resolutions (Figure 7).

An appropriate algorithm

Being interested only in using the maxima to estimate the parameters of magnetic sources, we must first attribute a maximum to either a thin-dike structure or a step-like structure (Figure 8). We assume the locations determined by the maxima of A_2 to be the magnetic boundaries. The amplitudes of A_1 and A_0 at the locations defined by A_2 are subsequently adopted to estimate the depth. If the location of a peak corresponds to

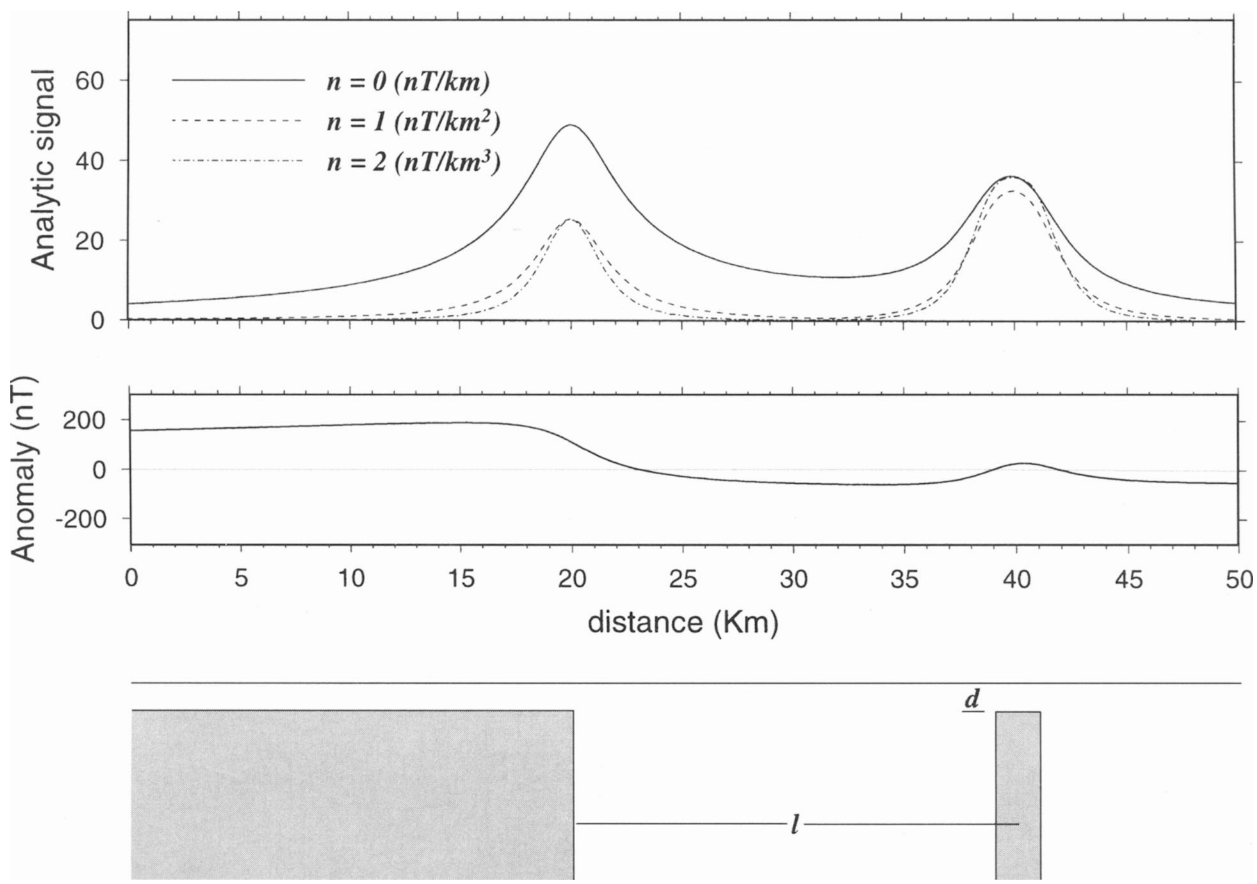

FIG. 5. Example showing the interference between a step and a thin-dike model. The depth to the top surface of each model is 2 km, while the bottom is at infinity. The inclination, declination, and intensity of magnetization for each model are $-5°$, $30°$, and 200 nT, respectively. There is only one maximum of the generalized analytic signal for the order $n = 0, 1, 2$ over the edge of the step model or the center of the thin-dike model.

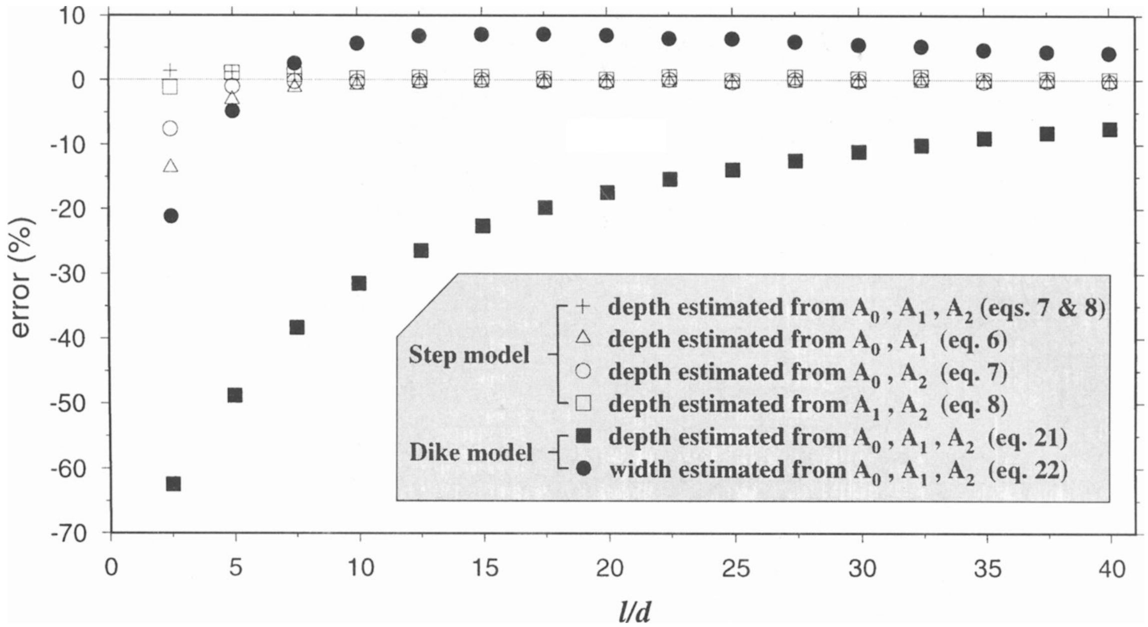

FIG. 6. Plot of the ratio of gap distance ℓ to depth d below the observation level versus the estimation error of geometric parameters of magnetic sources shown in Figure 5. The estimation is performed using the proposed amplitude ratio method.

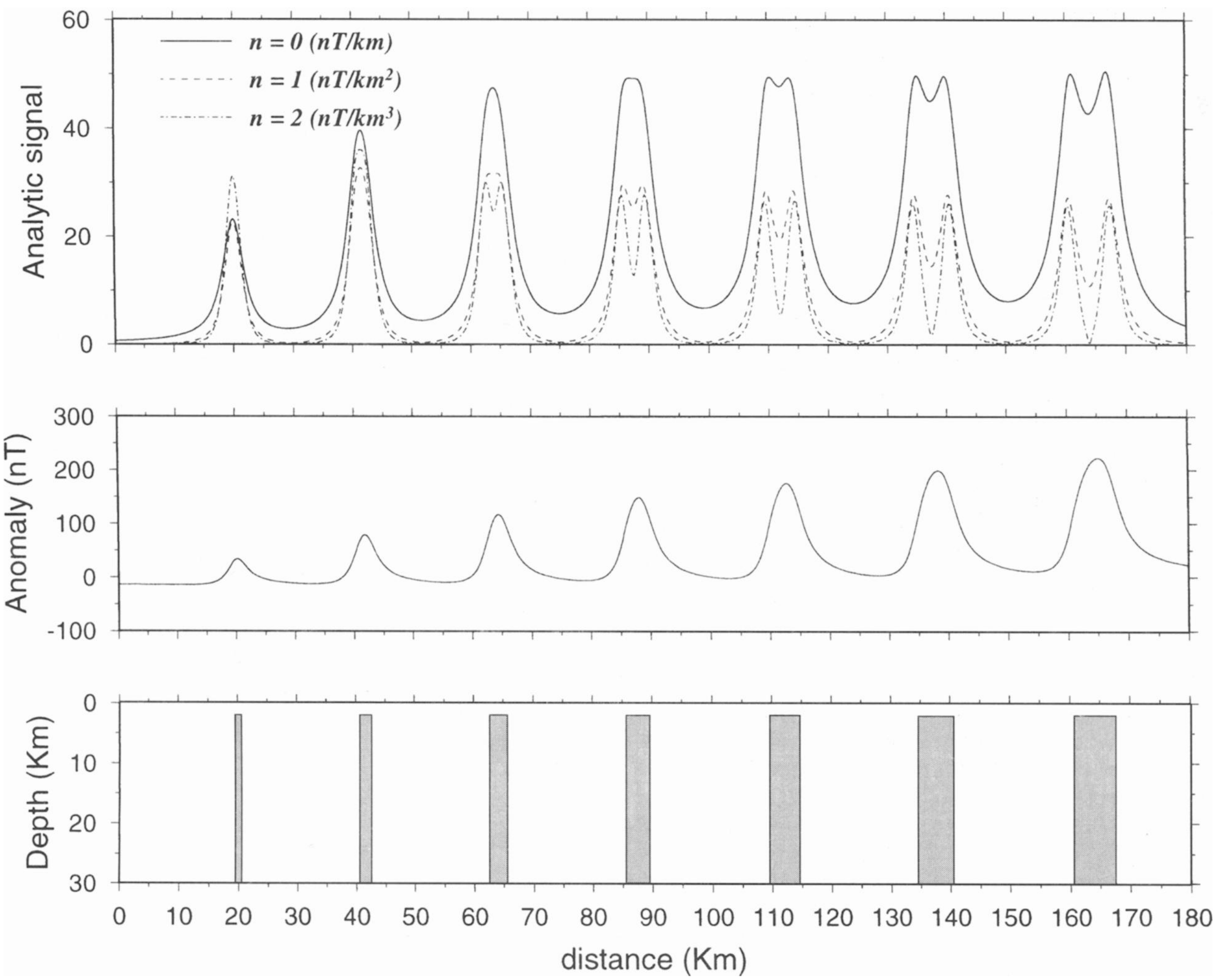

FIG. 7. Example showing the generalized analytic signal of dikes with varying widths from 1 to 7 km for the order $n = 0, 1, 2$. The parameters of magnetization are the same as in Figure 5. Note that a maximum could be located over the center of a thin dike or over either edge of a thick dike with some mislocation. The estimation of magnetic parameters is shown in Table 1.

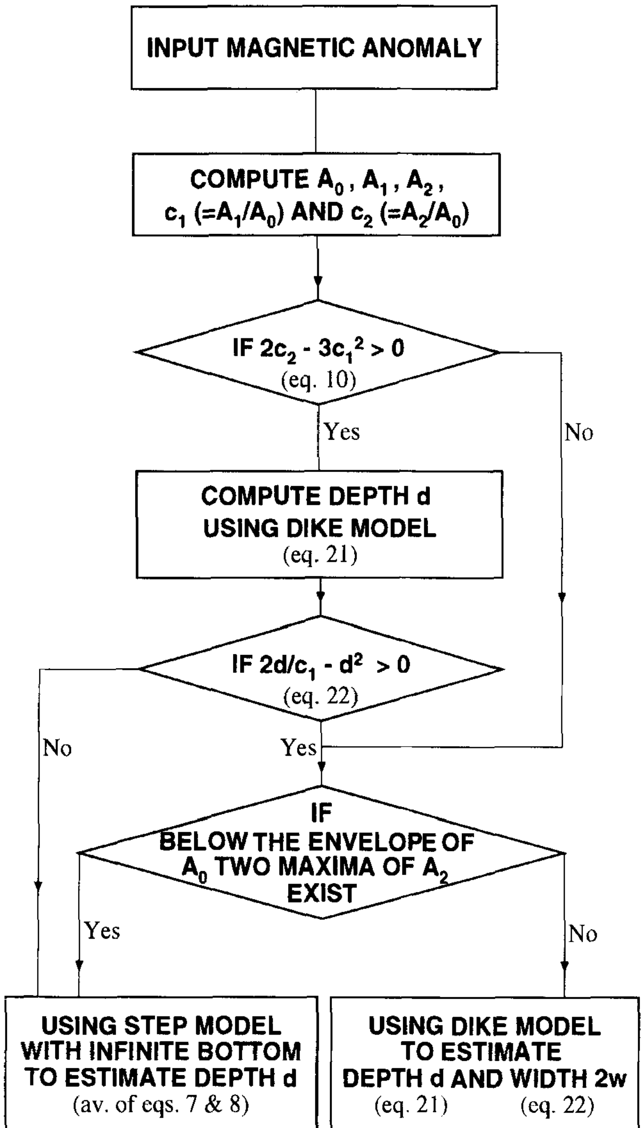

FIG. 8. An algorithm showing the optimal determination of magnetic depth from the amplitude ratio method.

the center of a dike, two new positions of boundaries could be given by adding or subtracting the estimated half-width of the dike, respectively.

Although the vertical step model, with finite thickness, yields a good depth estimation, it fails to yield a solution for a dike-like structure when $2c_2 - 3c_1^2 < 0$ (e.g., $2w \leq 4$ km) (Figure 7 and Table 1). Furthermore, when dikes are not very wide, the depth estimates are worse than the average depths estimated from equations (7) and (8) (e.g., 5 km $\leq 2w \leq$ 7 km). In contrast, the depth estimated from the dike model is not valid when $2w \geq 5$ km and the estimation errors become large in the ambiguous zone ($2w = 3$ km and $2w = 4$ km). In general, the optimal estimation for the magnetic parameters should be the values shown in the shaded area in Table 1. The depth of a dike is always underestimated if we interpret its analytic signal maximum on the basis of a step model; on the other hand, the depth of a contact is overestimated on the basis of a dike model (Table 1).

MAGNETIC DATA OFF SHORE NORTHERN TAIWAN

To demonstrate a practical application, we used magnetic data acquired offshore near northern Taiwan (Figures 9 and 10). The survey area is about 17×25 km^2, and the interval between profiles is about 1 km. The ship was navigated using GPS location. The earth's main field was removed from the data using the IGRF 1995 model (IAGA, 1996), and the diurnal variation was removed on the basis of geomagnetic data measured at a nearby observatory in Taiwan. A very strong magnetic anomaly occurs in the southern corner of the survey area (Figure 10) and correlates with the Pleistocene Chilung volcanoes (Ho, 1988). The relatively low magnetic anomaly in the southwestern portion of the survey area directly located at the offshore of the Chinshan delta (labeled C.D. in Figure 10) may suggest the northwest extension of the delta into the sea.

Northern Taiwan and its offshore area generally display northeast–southwest and northwest–southeast structural patterns. The northeast–southwest structures probably are linked to the formation of the Okinawa trough (Sibuet and Hsu, 1997), and the northwest–southeast structures (indicated by white arrows in Figure 10) are probably associated with the collision of the Luzon arc (e.g., Lu and Malavielle, 1994; Hsu et al., 1996a). The two pronounced faults in northern Taiwan (i.e., the Chinshan and Kanchiao faults) trend northeast–southwest (Figure 10). These are thought to be thrust faults dipping southeastward which are currently in an extensional environment

Table 1. Optimal estimation (values in shaded areas) for the parameters existing in Figure 7.

Parameter	Equation used	Value (km)	Value (km)	Value (km)	Value (km)	Value (km)	Value (km)	Value (km)
d	—	2	2	2	2	2	2	2
d_k	21	1.76	1.83	2.39	2.96	X	X	X
d_f	10	X	X	X	X	2.46	2.26	2.19
d_s	7 & 8	1.45	1.81	1.84	1.96	2.00	2.00	2.02
$2w$	—	1	2	3	4	5	6	7
$2w_e$	22	1.44	2.08	2.8 ± 0.2	3.8 ± 0.2	5.0 ± 0.2	6.2 ± 0.2	7.0 ± 0.2

X = invalid estimate
d = depth of each dike
d_k = depth estimated from a dike model
d_f = depth estimated from a vertical step model
d_s = depth estimated from a step model with infinite bottom surface [the average depth estimated from equations (9) and (10)]
$2w$ = width of each dike
$2w_e$ = width estimated from a thin-dike model or the distance between two edges of two step models

(e.g., Yeh et al., 1991; Chen et al., 1995; Hsu and Sibuet, 1995). The continuation of these two features offshore is suggested by bathymetric analysis (Liu et al., 1998).

The magnetic anomalies were gridded at a 0.5-km spacing before computing the analytic signal of the order $n = 0, 1, 2$. To avoid large high-frequency errors, the magnetic data were continued upward to 800 m above the sea's surface. The locations of the maxima of the second-order analytic signal, with indices greater than two, were determined by the method of Blakely and Simpson (1986). At each location, a step or dike structure and its corresponding depth were determined by using the algorithm shown in Figure 8 (Figure 11d). In addition, directional analysis was done at each maximum to show the strike of each structure. Generally, a linear continuation of the maxima with the same structural type suggests more credible solutions because the estimation discrepancy from the assumption of infinite strike length is not considered. Because of lack of borehole data, we could compare our results only with the solutions from the Euler deconvolution method (Thompson, 1982; Reid et al., 1990). The locations calculated from the Euler deconvolution method are more diffusive. However, the solutions with better convergence are quite consistent with the maxima of the analytic signal (cf. Figure 11a and 11c). The depth estimations from both methods are similar (cf. Figure 11c and 11d).

An example of where our method seems to be yielding results superior to the Euler deconvolution method can be seen at location *a* in Figure 11d. The analytic signal ratio solutions indicate a step structure, whereas the Euler deconvolution solutions are diffusive and unclear. This step-like structure agrees with the existence of tilted faults confirmed by seismic data (Huang et al., 1992). The structures near location *b* indicate a dike trending northwest–southeast and a small dike trending east–west. The linear structure near *b* corresponds to a bathymetric ridge (Liu et al., 1998), which implies the occurrence of a linear intrusion. This intrusive dike seems to be truncated by the offshore prolongation of the Chinshan fault (cf. Figures 10 and 11). The depth estimation to the top of the dike is somewhat deeper from the amplitude ratio method than from the Euler deconvolution method. However, if we

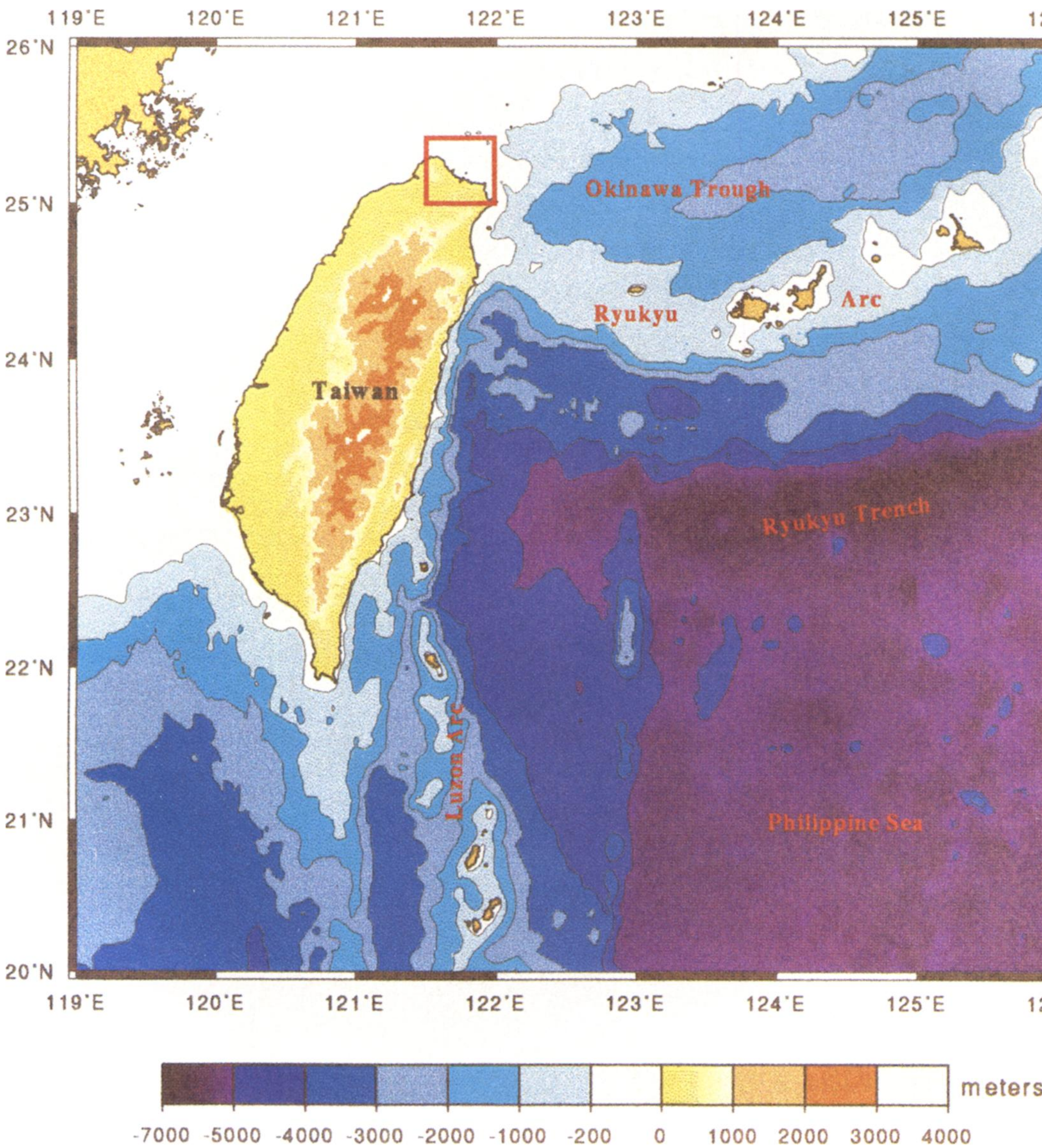

FIG. 9. The study area, indicated by the red box, located at the western end of the Okinawa trough. The southwestern Ryukyu arc and Okinawa trough have collided with the Luzon arc (Hsu et al., 1996b).

had used only the step model to interpret the analytic signal maxima in Figure 11a or 11b, we would have missed this intrusive structure. This demonstrates the major difference between this upgraded method and the one in Hsu et al. (1996b). A small islet (Chilunghsu), composed of Pleistocene quartizic andesite, is located to the southeast of the structure *b* (Figure 10) and displays strong analytic signal amplitudes (Figure 11b). Between Chilunghsu and structure *b*, a discrepancy in analytic signal exists and corresponds to the seaward extension of the Kanchiao fault (cf. Figures 9–11b). This interpretation can be easier done with an image view of the analytic signal in Figures 11a and 11b than just with a cluster of plotted symbols in Figure 11c by the Euler deconvolution method. As for the structure near *c*, the proposed method suggests a step model at a depth <0.5 km, which is in reasonable agreement with the Euler deconvolution results.

CONCLUSION

Based only on the maxima of the generalized analytic signal, an amplitude ratio method is developed to determine depth to magnetic source. It is assumed that magnetic sources can be characterized as dike-like and step-like structures. Using the amplitude ratios, we can discriminate between a dike-like or step-like structure. This capability is a significant improvement over earlier applications of analytic signal techniques, which used only the step model (Roest et al., 1992; Hsu et al., 1996b; Thurston and Smith, 1997). This implementation improves near-surface structural mapping of contacts and dikes. The amplitude ratio method does not require tedious operations with several characteristic points nor determination of the direction perpendicular to the strike of the structure.

This proposed method was applied to magnetic data acquired offshore northern Taiwan and shows the onshore Chinshan and Kanchiao faults extend seaward. A northwest–southeast-trending dike-like feature at depths <0.5 km is interpreted as a linear intrusion and seems to be associated with the occurrence of the Pleistocene Chilunghsu volcano. This dike-like feature and the Chilunghsu are probably cut by the seaward prolongation of the Kanchiao fault, resulting in a relatively low analytic signal in between.

ACKNOWLEDGMENTS

Constructive reviews from H. L. Yarger, A. H. Saad and M. Pilkington have greatly improved the old manuscript. H.-S. Yu, Y.-C. Chang, C.-S. Liu, and S.-Y. Liu provided useful data. C.-S. Lee kindly provided valuable references. This research was mainly supported by the National Science Council, Taiwan, under grants NSC 87-2611-M-002A-012-ODP and NSC87-2811-M002-0002.

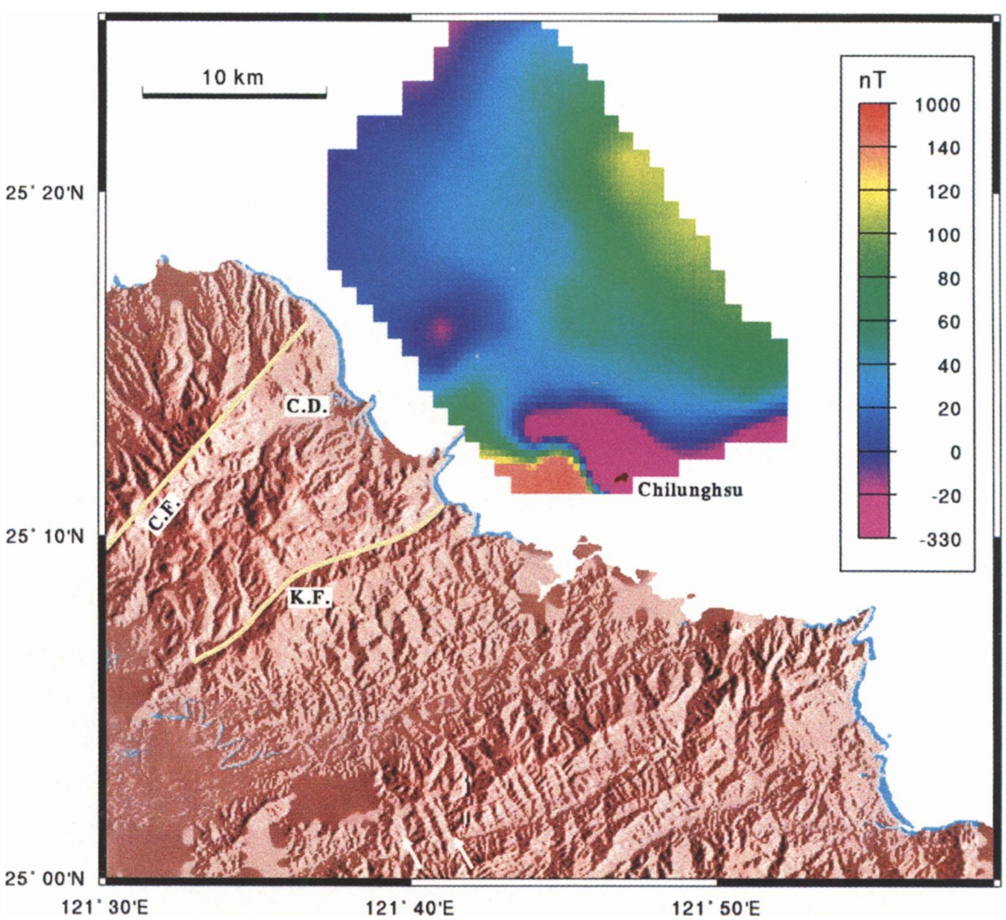

FIG. 10. Magnetic anomalies off northern Taiwan. The digital terrain model of northern Taiwan is plotted. C.F. = Chinshan fault, K.F. = Kanchiao fault, C.D. = Chinshan delta.

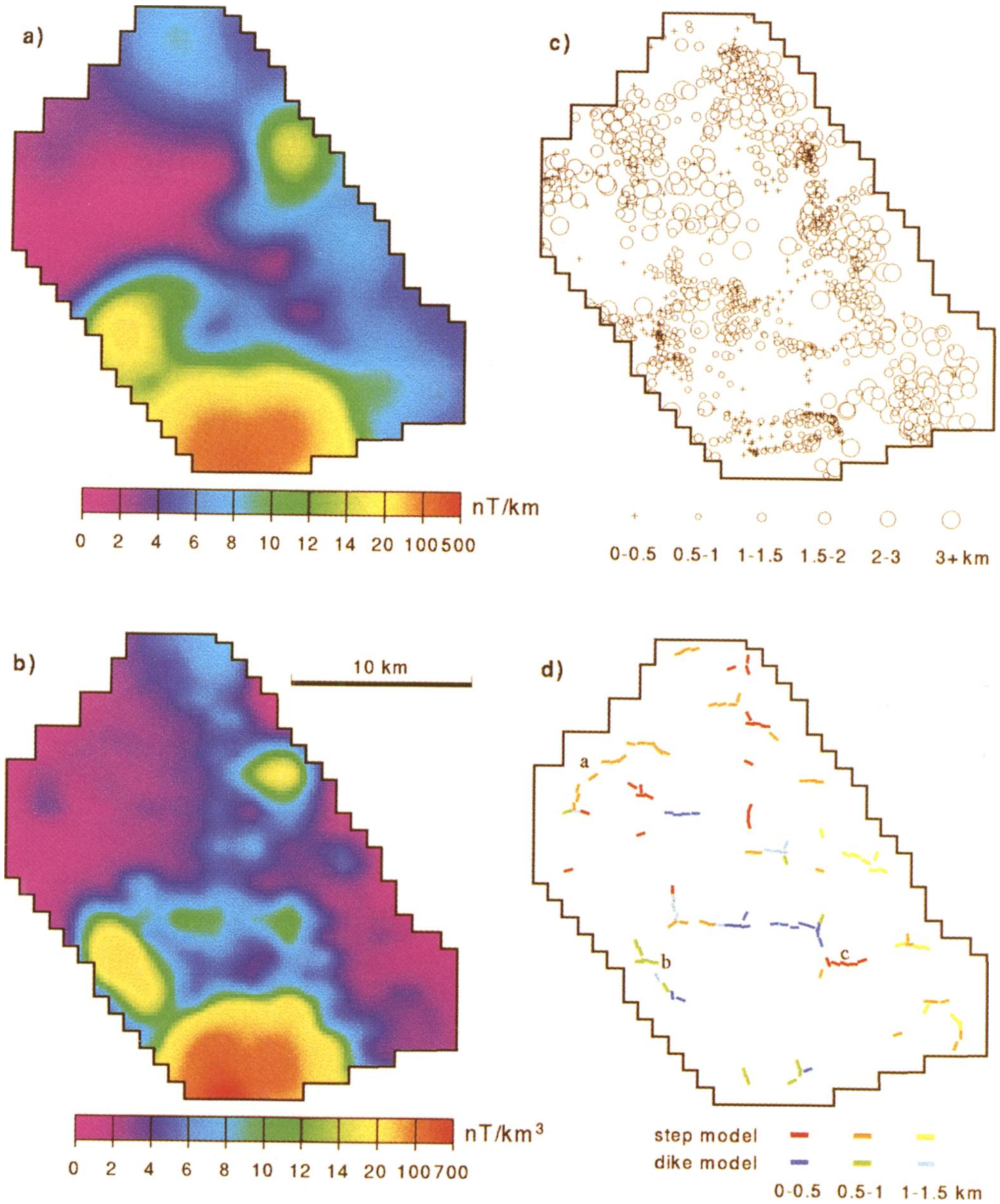

FIG. 11. (a) Amplitudes of the simple analytic signal ($n = 0$) of the magnetic anomalies shown in Figure 10 at 800 m above the sea surface. (b) Amplitudes of the second-order analytic signal ($n = 2$) of the magnetic anomalies shown in Figure 9b at 800 m above the sea surface. (c) The calculated depths by the Euler deconvolution method with the structural index $N = 0.5$, the window size of 7×7, and the acceptance level of 3% for the magnetic anomalies shown in Figure 10. (d) The depths to the top for either a step-like or a dike-like structure, determined by using the amplitude ratio method.

REFERENCES

Atchuta Rao, D., Ram Babu, H. V., and Sanker Narayan, P. V., 1981, Interpretation of magnetic anomalies due to dikes: The complex gradient method: Geophysics, **46**, 1572–1578.

Blakely, R. J., and Simpson, R. W., 1986, Approximating edges of sources bodies from magnetic or gravity anomalies: Geophysics, **51**, 1494–1498.

Chen, K.-J., Yeh, Y.-H., Yen, H.-Y., and Lin, C.-H., 1995, Seismological studies in the Chinshan fault area: J. Geol. Soc. China, **38**, 335–353.

Debeglia, N., and Corpel, J., 1997, Automatic 3-D interpretation of potential field data using analytic signal derivatives: Geophysics, **62**, 87–96, 1346.

Ho, C.-S., 1988, An introduction to the geology of Taiwan: Explanatory text of the geologic map of Taiwan, 2nd Ed.: Ministry Econ. Affairs, Rep. China.

Hsu, S.-K., and Sibuet, J.-C., 1995, Is Taiwan the result of arc-continent or arc-arc collision: Earth Planet. Sci. Lett., **136**, 315–324.

Hsu, S.-K., Sibuet, J.-C., Monti, S., Shyu, C.-T., and Liu, C.-S., 1996a, Transition between the Okinawa trough backarc extension and the Taiwan collision: New insights on the southermost Ryukyu subduction zone: Mar. Geophys. Res., **18**, 163–187.

Hsu, S.-K., Sibuet, J.-C., and Shyu, C.-T., 1996b, High-resolution detection of geologic boundaries from potential-field anomalies: An enhanced analytic signal technique: Geophysics, **61**, 373–386.

Huang, S.-T., Ting, H.-H., Chen, R.-C., Chi, W.-R., Hu, C.-C., and Shen, H.-C., 1992, Basinal framework and tectonic evolution of offshore northern Taiwan: Petro. Geol. Taiwan, **27**, 153–168.

International Association of Geomagnetism and Aeronomy (IAGA) Division V, Working Group 8, 1996, International geomagnetic reference field, 1995 revision: Geophys. J. Int., **125**, 318–321.

Liu, C.-S., Wang, C., Wang, S.-L., and Hsu, M.-K., 1997, A study of topographic features in the nearshore area of northern Taiwan, Acta

Oceanographica Taiwanica, **36**, 139–157.
Lu, C.-Y., and Malavielle, J., 1994, Oblique convergence, indentation and rotation tectonics in the Taiwan mountain belt: Insights from experimental modelling: Earth Planet. Sci. Lett., **121**, 477–494.
MacLeod, I. N., Jones, K., and Dai, T. F., 1993, 3-D analytic signal in the interpretation of total magnetic field data at low magnetic latitudes: Expl. Geophys., **24**, 679–688.
Marson, I., and Klingele, E. E., 1993, Advantages of using the vertical gradient of gravity for 3-D interpretation: Geophysics, **58**, 1588–1595.
Murthy, I. V. R., 1985, Magnetic interpretation of dike anomalies using derivatives: Pageoph, **123**, 232–238.
Nabighian, M. N., 1972, The analytic signal of two-dimensional magnetic bodies with polygonal cross-section: Its properties and use for automated anomaly interpretation: Geophysics, **37**, 507–517.
——— 1974, Additional comments on the analytic signal of two-dimensional magnetic bodies with polygonal cross-section: Geophysics, **39**, 85–92.
——— 1984, Toward a three-dimensional automatic interpretation of potential field data via generalized Hilbert transforms: Fundamental relation: Geophysics, **49**, 957–966.
Reid, A. B., Allsop, J. M., Granser, H., Millett, A. J., and Somerton, I. W., 1990, Magnetic interpretation in the three dimensions using Euler deconvolution: Geophysics, **55**, 80–91.
Roest, W. R., Verhoef, J., and Pilkington, M., 1992, Magnetic interpretation using the 3-D analytic signal: Geophysics, **57**, 116–125.
Sibuet, J.-C., and Hsu, S.-K., 1997, Geodynamics of the Taiwan arc-arc collision: Tectonophysics, **274**, 221–251.
Sundararajan, N., Mohan, N. L., Raghava, M. S. V., and Seshagiri Rao, S. V., 1985, Hilbert transform in the interpretation of magnetic anomalies of various component due to a thin infinite dike: Pageoph, **123**, 557–566.
Thurston, J. B., and Smith, R. S., 1997, Automatic conversion of magnetic data to depth, dip, and susceptibility contrast using the SPI(TM) method: Geophysics, **62**, 807–813.
Thompson, D. T., 1982, EULDPH: A new technique for making computer-assisted depth estimates from magnetic data: Geophysics, **47**, 31–37.
Yeh, Y.-H., Barrier, E., Lin, C.-H., and Angelier, J., 1991, Stress tensor analysis in the Taiwan area from focal mechanism of earthquakes: Tectonophysics, **200**, 267–280.